Singularity Analysis and Illustration of Inverse Kinematic Solutions of 6 DOF Fanuc 200IC Robot in Virtual Environment

Kamel Bouzgou, Zoubir Ahmed - foitih
Laboratory of Power
Systems, Solar Energy and Automation L.E.P.E.S.A
USTO. MB.Oran-Algeria
bouzgou_kamel@hotmail.fr, zfoitih@yahoo.fr

ABSTRACT: *In this paper, we demonstrate the analytical method for the solving of the inverse kinematics of 6 DOF manipulator arm, the FANUC 200IC, those solutions can be chosen after analysis of the Jacobian matrix, simplification and decomposition of this matrix leads us to solve a nonlinear equation with two variable, that we will limit the number of solution found, and that will give us the real workspace of robotaccessible by the end-effector. We validate our work by conducting a simulation software platform that allows us to verify the results of manipulation in a virtual reality environment based on VRML and Matlabsoftware, integration with the CAD model.*

Keywords: Forward Geometric Model, Inverse Kinematic Model, Singularity, Jacobian Matrix, 6 DOFmanipulator Arms, VRML, Matlab, Nonlinear Equation

Received: 10 June 2014, Revised 28 July 2014, Accepted 4 August 2014

1. Introduction

In telerobotic,the current problem of robotic systems has resulted in the reduction of physical workload of the operator, coupled with an increase in mental load.

To carry out a teleoperation action, it's necessary to provide the operator in the command/control situation, information on the progress of the task in the worksite, i.e. An assistance to the operator for perception, decision and control. That largely explains the development of the current artificial assistance techniques.

The purpose of this paper, is to present the results of a graphical simulation of robot control industrial manipulator Fanuc 6 DOF in an environment with a synthetic representation of the scene (virtual world), which consists of all relevant objects models from the task site.

Updating and animating of this virtual world, based on new mathematical techniques resulting from human reasoning field.

Initially, the robot was programmed and modeled by the manufacturer, with opaque and limited software for possible extensions.

For our use,we will try to develop a software model to an open system using the Matlab mathematical software in a virtual reality

(VRML).We will determine the boundaries of the work-space of the robot arm, that are defined by the mechanical articulation limits and by singularities [1, 2], several studies on this subject have been made [10, 11], For this we proceed by a theoretical study of the robot in order to identify geometric parameters, to determine the geometric and kinematic models required to our study.

2. Description of the Geometry of Fanuc 200ic Robot

The kinematics of the wrist is a RRR type, has three revolute joints with intersecting axes, equivalent to a ball socket (Figure 1).

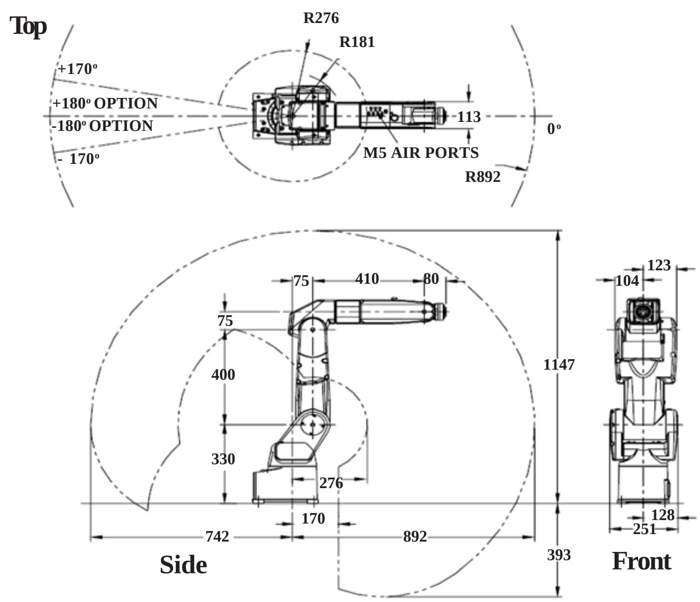

Figure 1. Dimension of the robot and the workspace. [4]

$d2 = 75 d3 = 400 d4 = 75$

$R4 = 410 R6 = 80$

From a methodological viewpoint, firstly we place Z_j axes on the joint axes, then the X_j axes, the geometric parameters of the robot are determined. The placement of frames is shown in Figure (Figure 2).

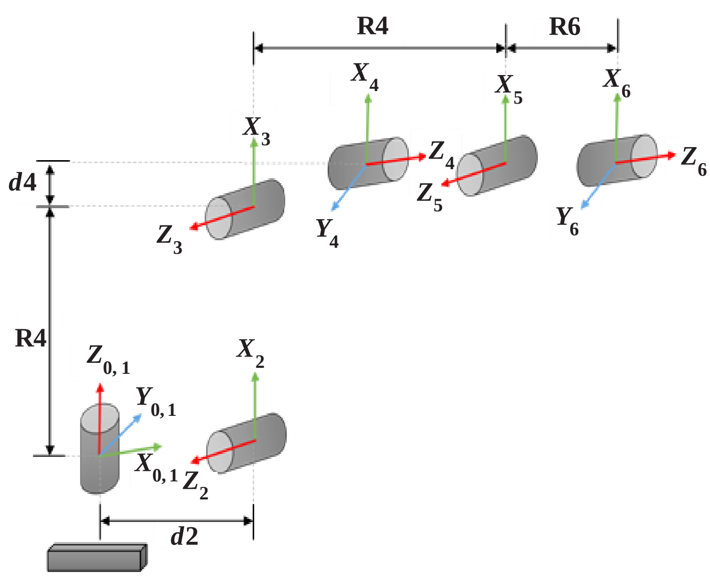

Figure 2. Real and complete architecture of FANUC robot

Axes 4, 5 et 6 are concurrent axes, they presented the orientation of the end-effector, and they don't affect its position, for this, we can be defined a E matrix that represents the translation of the coordinate system frame of the end-effector relative to the R_6 frame, this translation along the z axis is equal to $R_6 + r$, such that is the length along the same axis of the terminal member attached to the tool (e.g. A clamp) figure 3.

So, we get the modified following sch

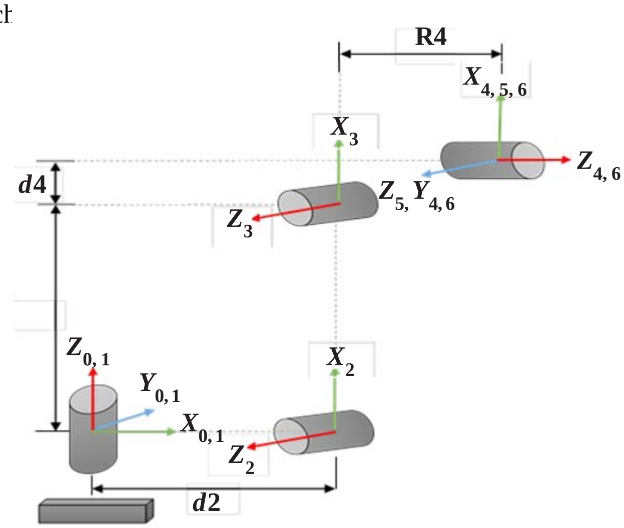

Figure 3. Architecture of the FANUC robot with Intersecting Axes

• The Passing from $Z_1 \rightarrow Z_2$ is done with a $\frac{\pi}{2}$ rotation angle, around x_1 axis,therefore the angle $a_2 = \frac{\pi}{2}$

• The passing from $x_1 \rightarrow x_2$ is done with $\frac{\pi}{2}$, around Z_2 axis [1].These passages are illustrated in the figure Figure 4.

Thus:

The initial position of x_2 (the robot is in rest) corresponds to $\frac{\pi}{2} + \theta_2$ angle (with $\theta_2 = 0$ in rest) therefore θ_2 (in motion) becomes: θ_2 receives $\theta_2 + \frac{\pi}{2}$.

joint j	σ_j	α_j	d_j	θ_2	R_j
1	0	0	0	θ	0
2	0	90	$d2$	$\frac{\pi}{2} + \theta_2$	0
3	0	0	$d3$	θ_3	0
4	0	90	$d4$	θ_4	R4
5	0	–90	0	θ_5	0
6	0	90	0	θ_6	0

Tableau 1. Modified geometric parameters D-H of the FANUCrobot. [8]

3. Geometric Model of the FANUC Robot

The homogeneous transformation matrices:

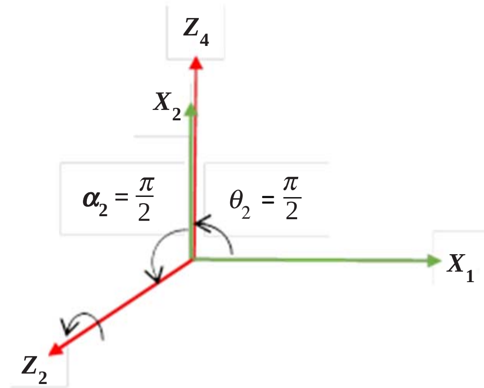

Figure 4. Elementary Rotation of axes

$$^0T_1 = \begin{bmatrix} C1 & -S1 & 0 & 0 \\ S1 & C1 & 0 & 0 \\ 0 & 0 & 1 & 0 \\ 0 & 0 & 0 & 1 \end{bmatrix} \qquad ^1T_2 = \begin{bmatrix} -S2 & -C2 & 0 & d2 \\ 0 & 0 & -1 & 0 \\ C2 & S2 & 1 & 0 \\ 0 & 0 & 0 & 1 \end{bmatrix}$$

$$^2T_3 = \begin{bmatrix} C3 & -S3 & 0 & d3 \\ S3 & C3 & 0 & 0 \\ 0 & 0 & 1 & 0 \\ 0 & 0 & 0 & 1 \end{bmatrix} \qquad ^3T_4 = \begin{bmatrix} C4 & -S4 & 0 & d4 \\ 0 & 0 & -1 & -S4 \\ 0 & 0 & 1 & 0 \\ 0 & 0 & 0 & 1 \end{bmatrix}$$

$$^4T_5 = \begin{bmatrix} C5 & -S5 & 0 & 0 \\ 0 & 0 & 1 & 0 \\ -S5 & -C5 & 0 & 0 \\ 0 & 0 & 0 & 1 \end{bmatrix} \qquad ^5T_6 = \begin{bmatrix} C6 & -S6 & 0 & 0 \\ 0 & 0 & -1 & 0 \\ S6 & C6 & 0 & 0 \\ 0 & 0 & 0 & 1 \end{bmatrix}$$

$$E = \begin{bmatrix} 1 & 0 & 0 & 0 \\ 0 & 1 & 0 & 0 \\ 0 & 0 & 1 & R6 \\ 0 & 0 & 0 & 1 \end{bmatrix}$$

Where: $C_i = cos\,(\theta_i)$

And $S_i = sin\,(\theta_i)$

3.1 Direct Geometric Model

The direct geometric model (DGM) is the set of relations which express the position of the end-effector, i.e. operational coordinates of the robot, according to its joint coordinates. In the case of a simple open-chain, it can be represented by the transformation matrix ^0T_k.

$$^0T_k = \prod_{i=1}^{k} {}^{i-1}T_i(q_i) \tag{2}$$

Realizing the composition of transformations universal frame R_0 until frame R_6 of equation (2) we obtain:

$$^0T_6 = {}^0T_1 . {}^1T_2 . {}^2T_3 . {}^3T_4 . {}^4T_5 . {}^5T_6 \text{ Let us note: } {}^fT_E = {}^0T_6 . E \quad (3)$$

$$^fT_E = \begin{bmatrix} s_x & n_x & a_x & p_x \\ s_y & n_y & a_y & p_y \\ s_z & n_z & a_z & p_z \\ 0 & 0 & 0 & 1 \end{bmatrix} \quad (4)$$

$E = {}^0T_E$: Transformation matrix of tool frame in the end-effector frame.

That is: $T = {}^0T_6 . E$

With:

$$\begin{cases} P_x = {}^fT_E\,(1, 4); \\ P_y = {}^fT_E\,(2, 4); \\ P_z = {}^fT_E\,(3, 4); \end{cases} \quad (5)$$

After calculation and identification of the terms of two matrices of the equation (3) (4), we will have:

$$^fT_E\,(1:3, 4) = T(1:3, 4)$$

$$\begin{cases} P_x = C1d2 + R6\,[C5C1C23 + S5(S1S4 - C4C1S23)] - d4C1S23 + R4C1C23 - C1S2d3 \\ P_y = d2S1 - d4S1S23 + R6\,[\,C5S1C23 - S5\,(C1S4 + C4S1S23)] + R4S1C23 - d3S1S2 \\ P_Z = C2d3 + d4C23 + R4S23 + R6\,[\,C5S123 + C4S523] \end{cases} \quad (6)$$

2. Inverse Kinematic Model

The inverse problem is to calculate the joint coordinates corresponding to a given situation of the end-effector. When it exists, the form which gives all the possible solutions constitutes what one calls the inverse kinematic model (IKM). We can distinguish three methods of calculating of:

- Paul's method. [10]
- Pieper's method. [9]
- General method of Raghavan& Roth.

Several iterative methods to find the IKM [6, 7] have been made, in our case, and analytical methods such as in [13], Pieper's method is suitable for manipulator arms with concurrent wrist axes are used.

2.1 Inverse Kinematic Model of FANUC Robot

$$U_0 = \begin{bmatrix} & & & P_x \\ & {}^0A_E & & P_x \\ & & & P_x \\ 0 & 0 & 0 & 1 \end{bmatrix} \quad (7)$$

With ^0A_E orientation matrixof frame R_E / R_0

2.1.1 Calculation of θ_1, θ_2 and θ_3

$$U_0 = {}^0T_6 \,.\, E$$

$$U_0 \,.\, E^{-1} = {}^0T_6$$

$$\grave{U}_0 = U_0 \,.\, E^{-1}$$

With $\grave{U}_0$ a new orientation matrix

$${}^1T_0 \,.\, \grave{U}_0 \,.\, [0\ 0\ 0\ 1]^T$$

Implies:

$${}^1T_0 \,.\, \grave{U}_0 \,.\, [0\ 0\ 0\ 1]^T = {}^1T_6 \,.\, [0\ 0\ 0\ 1]^T$$

And

$${}^1T_0 \,.\, \grave{U}_0 \,.\, [0\ 0\ 0\ 1]^T$$

Implies:

$${}^1T_6 \,.\, [0\ 0\ 0\ 1]^T = {}^1T_4 \,.\, [0\ 0\ 0\ 1]^T$$

Because we have a three intersecting axes While using Matlab mathematical software we found:

$$\begin{cases} C1P_x + R6C1 + P_yS1 = d2 - d3S2 - d4S23 + R4C23 \\ R6S1 + C1P_y - P_xS1 = 0 \\ P_Z = C2d3 + d4C23 + R4S23 \end{cases} \tag{8}$$

With:

$$C23 = cos\,(\theta_2 + \theta_3)$$
$$S23 = sin\,(\theta_2 + \theta_3)$$

By using the 2nd equality of (8)

$$-S_1\,(P_x - R6) + C1P_Y = 0$$

Thus:

$$\begin{cases} \theta_1 = \mathrm{ATAN2}\,(P_y,\, P_x - R6) \\ \theta_1 = \theta_1 + \pi \end{cases} \tag{9}$$

From a 1st equality of (8) we make:

$$C1P_x - R6\mathrm{C}1 + P_yS_1 - d2 = A$$

And the all became

$$\begin{cases} A = d3S2 - d4S23 + R4C23 \\ P_z = C2d3 + d4C23 + R4S23 \end{cases} \tag{10}$$

From a 1st equality of (10) we draw $S2$

$$S2 = \frac{R4C23 - \mathrm{d}4\mathrm{S}23 - A}{d3} \tag{11}$$

From a 2nd equality of (10) we draw: $C2$

$$C2 = \frac{P_z - d4C23 + R4S23}{d3} \tag{12}$$

Therefore:

$$d3^2\, S2^2 = R4^2\, C23^2 + d4^2\mathrm{S}23^2 - 25R4d4C23S23 + A^2 - 2AR4C23 + 2Ad4S23$$

$$d3^2\, S2^2 = P_z^{\ 2} + d4^2\, C23^2 - 2P_zd4C23 + R4^2S23^2 + 2P_zR4S23 + 2R4D4C23S23$$

$$d3^2 = C23^2\,[R4^2 + d4^2] + S23^2\,[R4^2 + d4^2] + C23\,[-2AR4 - 2P_zd4] + S23\,[2Ad4 - 2P_zR4] + P_z^{\ 2} \tag{13}$$

We pose
$$X = -2AR4 - 2P_z d4$$
$$Y = 2Ad4 - 2P_z R4$$
$$H = R4^2 + d4^2 + P_z^{\,2} - d3^2 + A^2$$
We replace in (13):
$$XC23 + YS23 + H = 0$$
$$-YS23 = XC23 + H$$
$$Y^2 - Y^2C23^2 = X^2C23^2 + 2XHC23 + H^2$$
$$(X^2 + Y^2)\,C23^2 + 2XHC23 + (H^2 - Y^2) = 0$$
Equation (According to $C23$) of the second degree admits two real solutions if $\Delta \geq 0$ with:
$$\Delta = (2XH)^2 - 4\,(X^2 + Y^2)\,(H^2 - Y^2) \text{ Thus:}$$
$$C23 = \frac{-2XH \pm \sqrt{\Delta}}{2(X^2 + Y^2)}$$
$$S23 = \sqrt{1 - C23^2}$$
We replace its in (11) and (12) we find:
$$\begin{cases} \theta_2 - ATAN2\,(S2, C2) \\ \theta_3 = ATAN2\,(S23, C23) - \theta_2 \end{cases} \tag{14}$$

2.1.2 Calculation of θ_4, θ_5 and θ_6

We have found θ_1, θ_2 and θ_3; therefore the matrix ${}^0T_3$ is known:
$$U_0 = {}^0T_6 \Rightarrow {}^3T_0\,U_0 = {}^3T_6$$
$${}^4T_3\,{}^3T_0\,U_0 = {}^4T_6 = \begin{bmatrix} {}^4A_6 & & & P \\ 0 & 0 & 0 & 1 \end{bmatrix}$$
$${}^3T_6\,U_0 = \begin{bmatrix} V_{11} & V_{12} & V_{13} & V_{14} \\ V_{21} & V_{22} & V_{23} & V_{24} \\ V_{31} & V_{32} & V_{33} & V_{34} \\ 0 & 0 & 0 & 1 \end{bmatrix}$$
$$M = {}^4T_3\,{}^3T_0\,U_0$$
$$M = \begin{bmatrix} C4V_{13} + S4V_{13} & - C4V_{12} - S4V_{32} & C4V_{11} + S4V_{31} \\ C4V_{33} - S4V_{13} & - C4V_{32} + S4V_{12} & C4V_{31} - S4V_{11} \\ -V_{23} & V_{22} & -V_{21} \end{bmatrix}$$
$${}^4A_6 = \begin{bmatrix} C5C6 & -C5C6 & S5 \\ S6 & C6 & 0 \\ -C6C5 & S5S6 & C5 \end{bmatrix}$$

$$^{0}A_6 = (2, 3) = 0;\ M(2, 3) = C4_{31} - S4V_{11}$$

So by identifying:

$$C4V_{31} = S4V_{11}$$

$$\frac{S4}{C4} = \frac{V_{33}}{V_{11}}$$

$$\begin{cases} \theta_4 = ATAN2\,(V_{31}, V_{11}) \\ \theta_4 = \theta_4 + \pi \end{cases} \qquad (15)$$

$$M(3, 3) = -V_{21}$$

$$^{0}A_6\,(3, 3) = C5$$

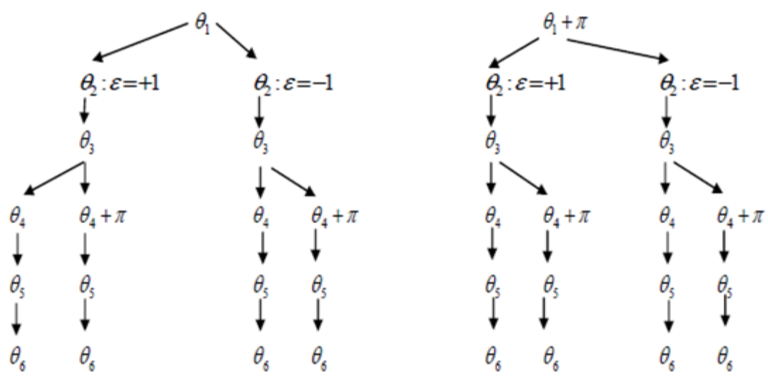

Figure 5. Tree structures of solutions of the IKM

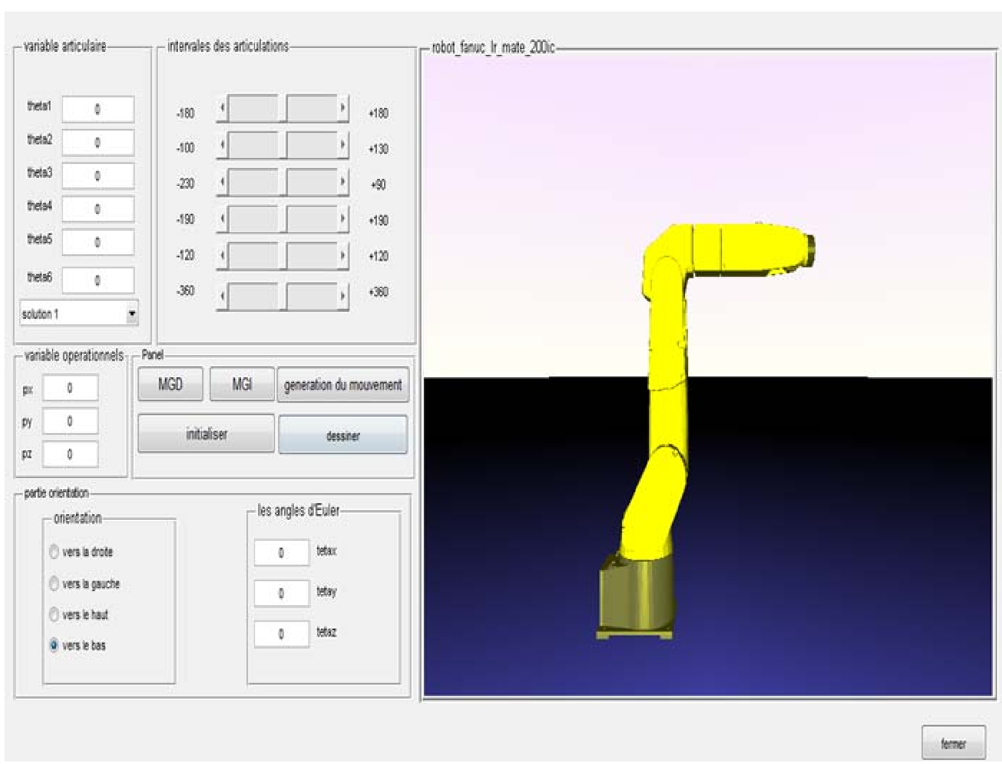

Figure 6. Main Interface

$$M(1,3) = C4V_{11} + S4_{31}\,{}^{4}A_{6}(1,3) = S5 \tag{16}$$

$$\theta_5 = ATAN2(M(1,3), M(3,3))$$

$$M(2,1) = C4V_{33} - S4V_{13}\,{}^{4}A_{6}(2,1) = S6$$

$$M(2,2) = -C4V_{32} - S4V_{12}\,{}^{4}A_{6}(2,2) = C6$$

Thus

$$\frac{S6}{C6} = \frac{M(2,1)}{M(2,2)}$$

$$\theta_6 = ATAN2(M(2,1), M(2,2)) \tag{17}$$

We will have up to 8 solutions outside the singular positions; some of these configurations may not be accessible because of joint limits. An illustration of these 8 solutions is represented by Figure 5.

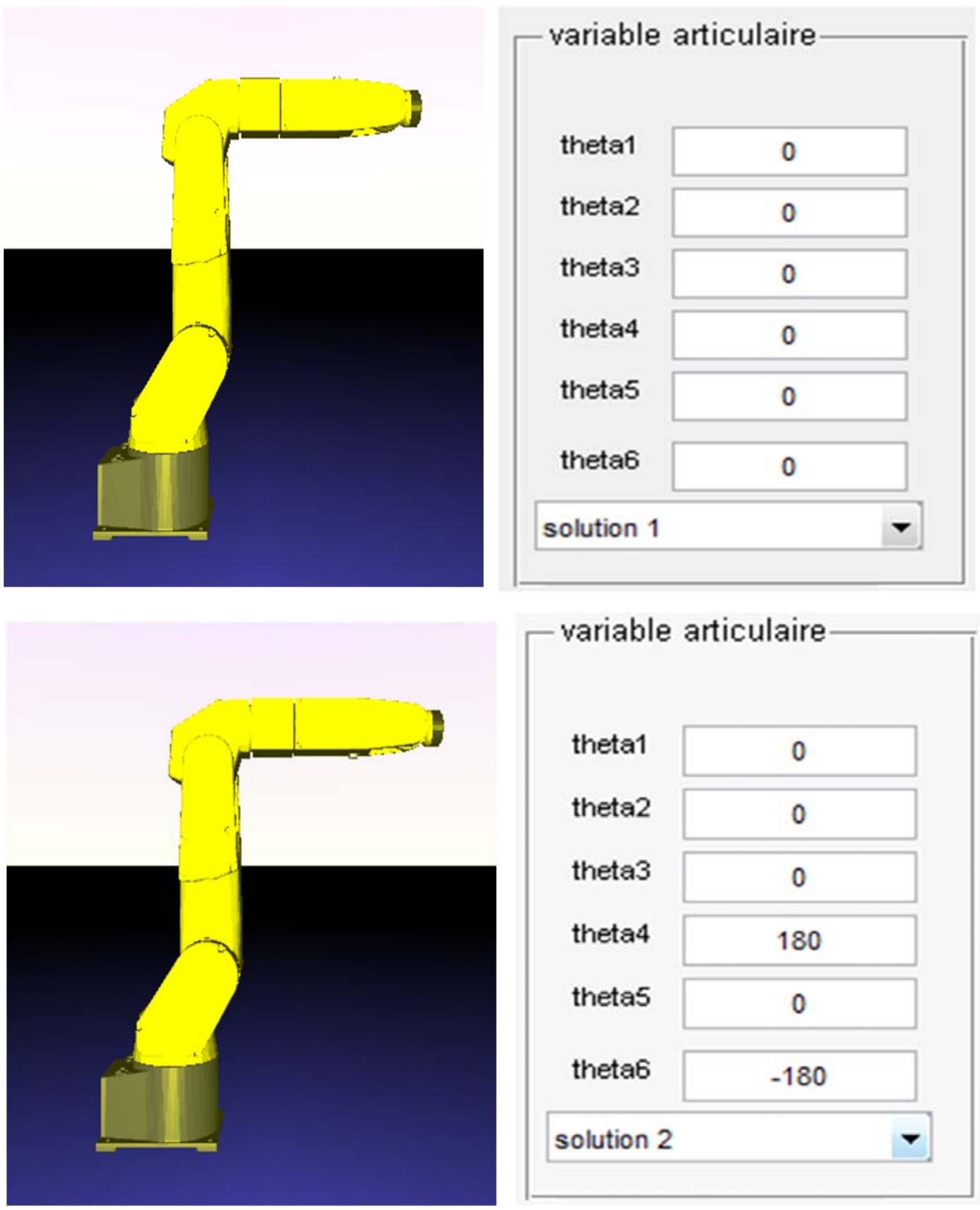

2.1.3 Eight Solutions Corresponding to a Given Configuration

We developed for this study a graphical interface with Matlab,where we integrated the robot designed with CAD [5] in the application under VRML for visualizing well and to handle the arm, figure 6 shows the general pace of this interface.

We choose as a configuration of demonstration, the initial position of the arm manipulator such as: $p_x = 565$, $p_y = 0$, $p_z = 475$.

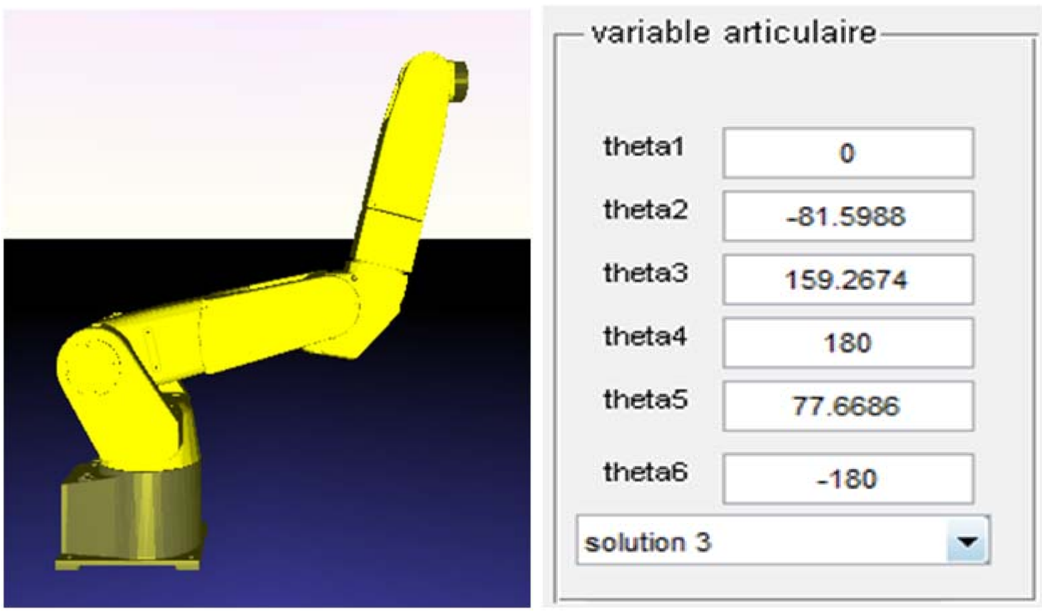

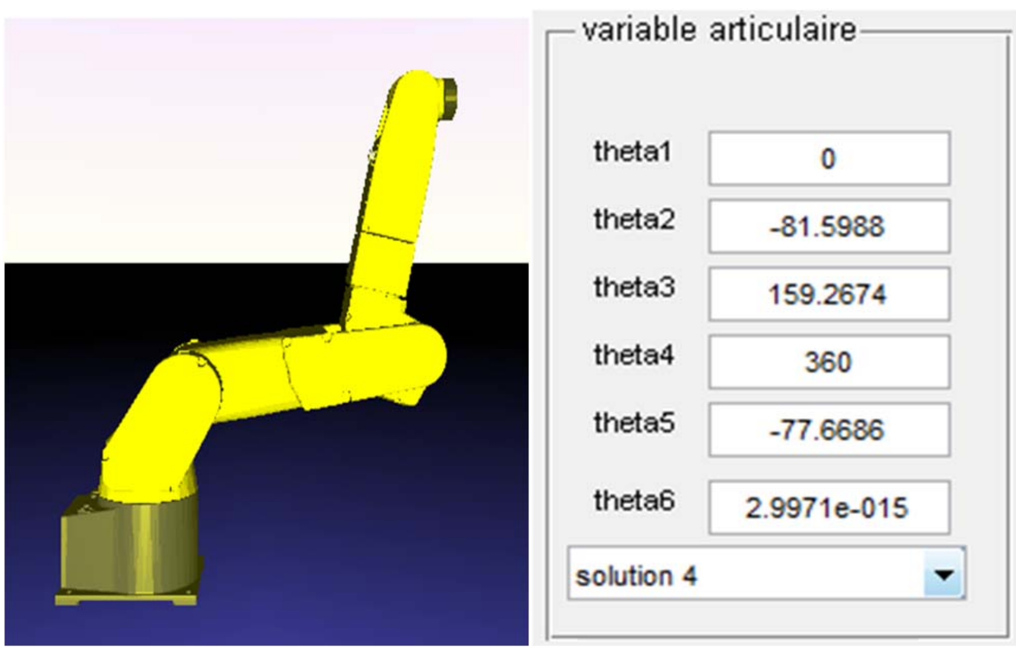

3. Singularities of FANUC Robot

We can find singularities from any Jacobian matrix, but we often choose the projection of the ${}^6J_6$ matrix in the R_i reference frame which gives us the simplest ${}^iJ_6$ matrix. [1]

Sothe J^{th} column of ${}^6J_6$ Jacobian matrix is:

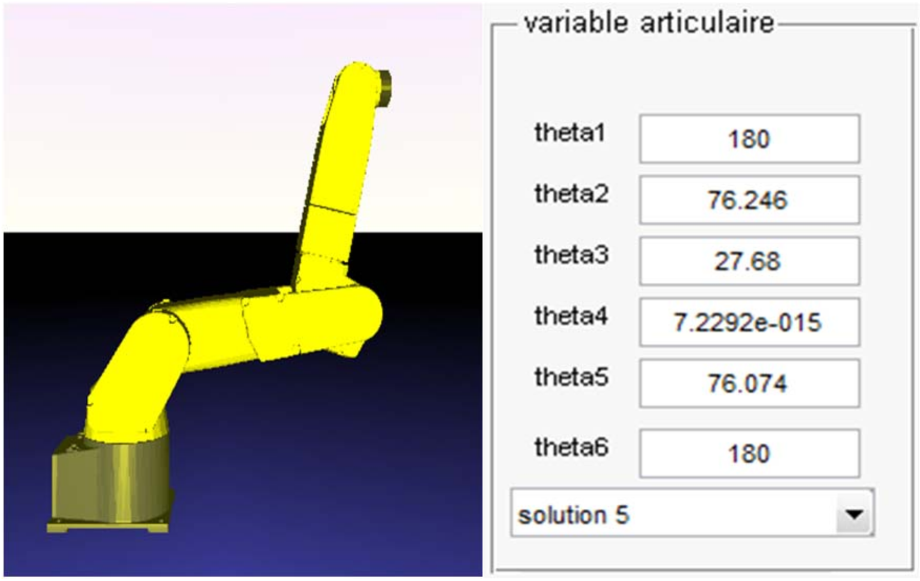

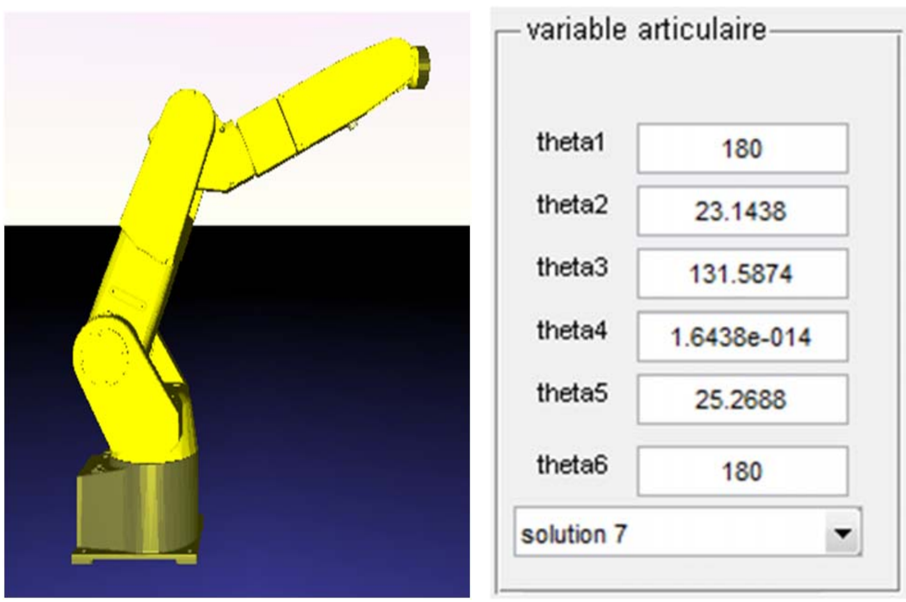

$$ {}^6J_j = \begin{bmatrix} {}^6A_j\left[\begin{pmatrix}0\\0\\1\end{pmatrix}\wedge {}^jP_n\right] \\ {}^6A_j\begin{pmatrix}0\\0\\1\end{pmatrix}\end{bmatrix} $$

$$ {}^6J_j = \begin{bmatrix} -\begin{bmatrix}s_x\\n_x\\a_x\end{bmatrix}.P_y + \begin{bmatrix}s_y\\n_y\\a_y\end{bmatrix}.P_x \\ \begin{bmatrix}s_z\\n_z\\a_z\end{bmatrix}\end{bmatrix} \tag{18} $$

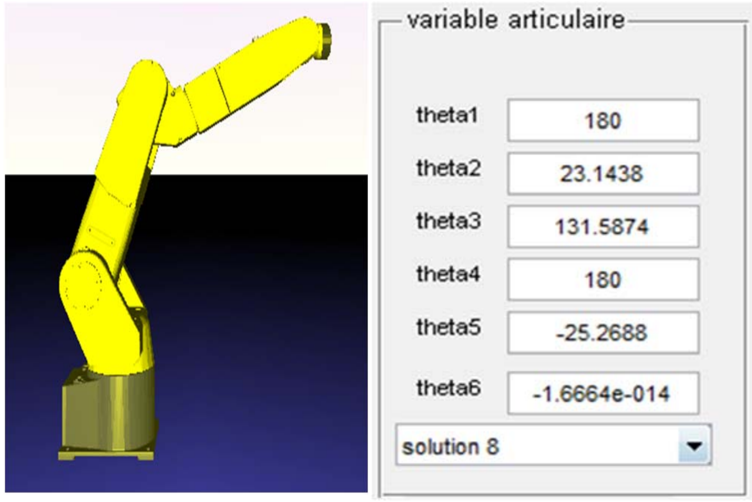

Figure 6. Illustration of the 8 solutions of IK in the VRML interface

In our case this matrix will be the projection of ${}^{3}J_{6}$ in the R_3 reference frame, thus we will obtain the Jacobian matrix ${}^{3}J_{6}$ which defines R_6 the reference frame in the R_3 frame.

The ${}^{3}J_{6}$ matrix has particular form as:

$$ {}^{3}J_{6} = \begin{bmatrix} A & 0_3 \\ B & C \end{bmatrix} \tag{19} $$

Where: A, B, C and 0_3 are matrices of (3×3)dimension.

$$ \det({}^{3}J_{6}) = \det(A).\det(C) \tag{20} $$

In order to calculate ${}^{3}J_{6}^{-1}$, It is necessary that $\det(J) \neq 0$Therefore:

$$ \det(A).\det(C) = 0 \Rightarrow \begin{cases} \det(A) = 0 \\ \quad ou \\ \det(C) = 0 \end{cases} \tag{21} $$

$$ \det(C) - S5C4^2 - S5S4^2 $$

$$ \det(C) = 0 \Rightarrow S5 = 0 $$

Figure 7. Singularity of wrist

Thus: $\theta_5 = 0$ or $\theta_5 = \pi$

$\theta_5 = \pi$, because of obstinate mechanics, θ_5 angle can be taking a first solution only, so $\theta_5 = 0$ Thus: det $(C) = 0 \Rightarrow \theta_5 = 0$ (22)

With this configuration, the two articulations and have their confused axes, which makes lose a degree of freedom to the robot, the rotation of the end-effector can be done is by the rotation ofor, the robot thus has practically 5 DOF.

$$\det(A) = d3[\,C3R4 - d4S3][d2 + d3S2 + C2C3R4 - C2d4S3 + C3d4S2 + R4S2S3]$$

$$= d3[\,C3R4 - d4S3][d2 + d3S2 + C2(R4C3 - d4S3) + S2\,(R4S3 + d4C3)\,]$$

$$\det(A) = 0 \begin{cases} d3[\,C3R4 - d4S3] = 0 \\ \quad or \\ d2 + d3S2 + C2(R4C3 - d4S3) + S2\,(R4S3 + d4C3) = 0 \end{cases} \tag{23}$$

$$C3R4 - d4S3 = 0 \Rightarrow \frac{S3}{C3} = \frac{R4}{d4}$$

Thus:

$$\begin{cases} \theta_3 = ATAN2\,(R_4, d_4) = 1.3899 \\ \theta_3 = \theta_3 + \pi = 4.5315 \end{cases} \tag{24}$$

$$d2 + d3S2 + C2\,(R4C3 - d4S3) + S2\,(R4S3 + d4C3) = 0 \tag{25}$$

That it becomes to solving a non-linear equation with two unknown θ_2, θ_3 analytically is difficult, we use the mathematical software Matlab to find the solutions geometrically:

We can display this result with a tablecloth of the three variables θ_1, θ_2 and 3:

This solution is purely mathematical because $\theta_2, \theta_3 \in [-\pi, +\pi]$, and as we have constraints at the articular space because: $(-1.7453 \leq 02 \leq 2.2689$ et $-4.0143 \leq 03 \leq 1.5708)$

figure 8 became as follows:

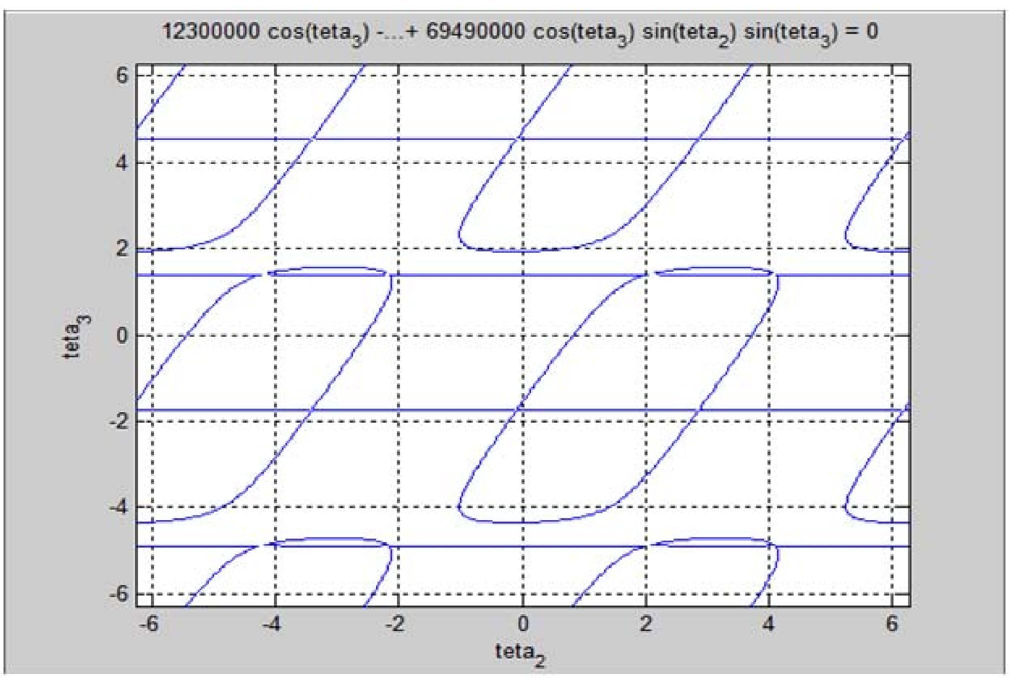

Figure 8. Branches of the singularities without butted in θ_2, θ_3 plan

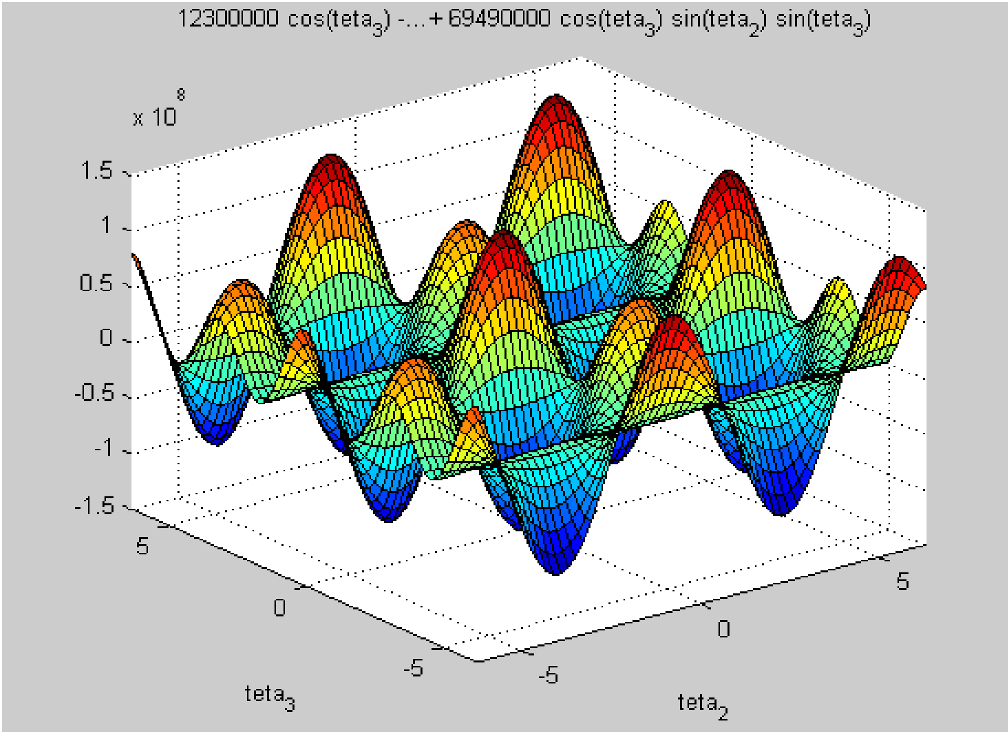

Figure 9. Surface of Singularities

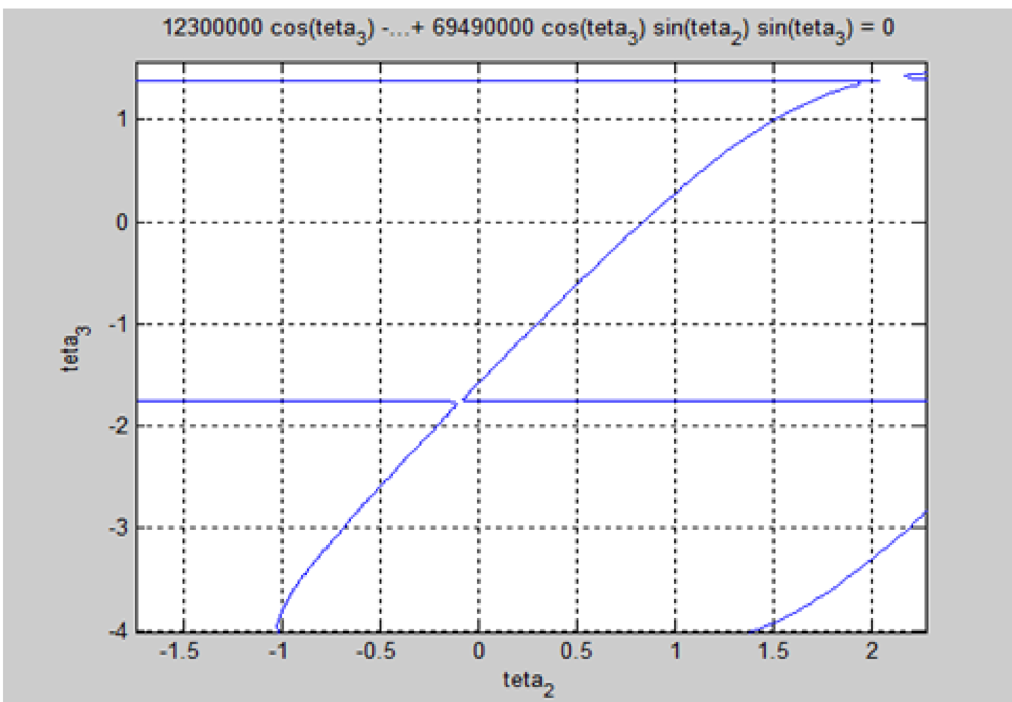

Figure 10.Singularities branche with buttes

5. Conclusion

The inverse kinematic model gives us the eight solutions of the positions of the end-effector apart from the singularities, we could visualize them in a virtual environment by using a software other than the manufacturer's software, the space work of the arm is limited by the articular thrusts and the branches of the singularities, which are represented in the form of curves and right-hand sides while solving an equation with two unknown. Several mathematical tools are used in this study, whose validation of our work was made using Matlab. We can thereafter consider other research orientations such as the generation of motion and the planning of trajectory [3].

References

[1] Khalil, W., Dombre, E. (1999). Modelisation identification et commande des robots 2nd edition.

[2] LALLEMAND, J. P. (1994). *Robotique Aspects fondamentaux*. Paris.

[3] Bouzgou, K., Bellabaci, M. A. Ahmed-Foitih, Z. Modélisation, commande et génération de mouvement du bras manipulateur FANUC 200Ic manipulateur FANUC 200iC, memoire Master informatique industrielle, 2012-2013.

[4] Récupéré sur FANUC Robotics: http://www.fanucrobotics.com.

[5] GRABCAD. Récupéré sur http://grabcad.com/

[6] Benhabib, B., Goldenberg, A. A., Fenton, R. G. (1985). A solution to the inverse kinematics of redundant manipulators, IEEE.

[7] Toyosaku, I., Nagasaka, K., Yainamoto, S. (1992). A New Approach to Kinematic Control ofSimple Manipulators, IEEE.

[8] Denavit, J., Hartenberg, R. S. (1995). A Kinematic Notation for Lowerpair Mechanisms Based on Matrices, *Journal of Applied Mechanics*.

[9] Pieper, D. L. (1968). The kinematics of manipulators under computer control, PhD thesis, Stanford university.

[10] Paul, R. C. P. (1981). Robot manipulators:Mathematics,programming and control, MIT press,Combridge.

[11] Vaezi, M., Jazeh, H.E.S. (2011). Singularity Analysis of 6DOF Stäubli© TX40 Robot, International Conference on Mechatronics and Automation, August 7 - 10, Beijing, China, IEEE.

[12] Djuric, A. M., Filipovic, M., Kevac, L. (2013). Graphical Representation of the Significant 6R KUKA Robots Spaces SISY 2013, IEEE 11th International Symposium on Intelligent Systems and Informatics, September 26-28, Subotica, Serbia.

[13] Gan, J. Q., Oyama, E., Rosales, E. M., Hu, H. (2005). A complete analytical solution to the inverse kinematics of the Pioneer 2 robotic arm, Robotica cambrige press.